Proceedings of the Combustion Institute, Volume 28, 2000/pp. 1917–1924

A COMPUTATIONAL STUDY OF THE TRANSITION FROM LOCALIZED IGNITION TO FLAME BALL IN LEAN HYDROGEN/AIR MIXTURES

S. D. TSE, L. HE AND C. K. LAW

Department of Mechanical and Aerospace Engineering Princeton University
Princeton, NJ 08544, USA

A computational study has been conducted to determine the critical conditions for the transition from localized flame ignition and propagation to the establishment of a flame ball. Lean H_2/air mixtures are investigated using a time-dependent, spherically symmetric code with detailed chemistry, transport, and radiation submodels. Results show that outwardly propagating spherical flames can be ignited for hydrogen mole fractions X_{H_2} larger than ~3.5%. Furthermore, assuming optically thin radiative heat loss, flame balls can be established from centrally ignited premixed spherical flames only within a narrow range of mixture compositions (i.e., $\sim 3.5\% < X_{H_2} < \sim 6.5\%$). For $\sim 6.5\% < X_{H_2} < \sim 11\%$, flames propagate until radiative extinction, never evolving into flame balls, while for $X_{H_2} > \sim 11\%$, the expanding spherical flames develop asymptotically into planar propagating flames. These findings corroborate the experimental result that the range of mixtures within which flame balls have been observed is much narrower than that predicted by previous one-dimensional instability analysis of the flame ball, where it was shown that steady flame balls exist for $3.5\% < X_{H_2} < 10.7\%$. The present simulation also shows that the dynamic transition from a spherically propagating flame to the flame ball controls the range of mixtures for which flame balls can be reached, with radiative loss being both the requisite mechanism for and the limiting mechanism against the dynamic transformation. Additional calculations show that the size of the flame ball is noticeably enlarged when radiative reabsorption is incorporated.

Introduction

Studies on outwardly propagating flames [1–3] have frequently assumed that the flame radius is much larger than the flame thickness such that both the structure and flame velocity are only slightly different from those of the planar flame. The structure of the stationary flame ball [4], however, is very different in that convective transport is absent while the product and heat release are diffusively transported outward to the ambient. As such, the flame structure assumes a diffusive character and is not localized. Stability analyses by Zeldovich et al. [5] and Deshaies and Joulin [6] through the thermal-diffusion model showed that the adiabatic stationary flame ball is unconditionally unstable at its equilibrium radius, tending to either collapse inward for a negative perturbation of the flame position or propagate outwardly for a positive perturbation. Based on such an unstable nature of the stationary flame ball, Zeldovich et al. [5] indicated that heat loss could play a stabilizing role because the extent of heat loss varies directly with the flame size. This concept was further developed by Buckmaster et al. [7,8], via asymptotic analysis, showing that, in the presence of heat loss in the near field, the solution with the smaller equilibrium radius is unstable to one-dimensional perturbations while that with the larger equilibrium radius is stable. It was thus suggested that the flame balls observed in experiments carried out in microgravity [9,10] were stabilized by heat loss and that flame balls can be observed only when the Lewis number is smaller than unity [11].

Non-adiabatic, *steady* flame balls in H_2/air mixtures with radiative loss were first numerically obtained by Buckmaster et al. [12] and Smooke and Ern [13]. The results were qualitatively consistent with the analytical theories, although the computed steady flame ball radii were up to a factor of 2 smaller than experimental observations. More recently, Wu et al. [14] computationally studied the transient responses of stationary flame balls perturbed from their steady-state structures, and stable stationary flame balls were predicted to exist up to 10.7% for H_2 in air, which is much higher than the experimentally observed concentration limit.

The present investigation was motivated by recognizing that in these previous studies the flame ball was considered as a particular phenomenon isolated from the propagating flame. In practical situations, however, a propagating spherical flame is first established when a localized ignition source of finite energy is deposited in a reactive mixture. As such, the existence of stable flame ball solutions does not mean that they are dynamically attainable from an initially established flame at ignition. It is reasonable to expect that the structure of this initial flame must be localized and hence very different from that of

the stationary flame ball, which extends out to infinity as $1/r$. Furthermore, arbitrary perturbations of a steady flame ball solution to the extent that the flame extinguishes do not define the only set of possible initial profiles for which it can be attained.

Recognizing the subtlety and importance of the above issues, and by using simplified chemical, thermodynamic, and transport properties, He and Law [15] theoretically and numerically showed that an expanding spherical flame degenerates to a flame ball only for sufficiently large heat loss. With decreasing heat loss, the spherical flame will either propagate until extinction if the loss is moderate or asymptotically approach the planar flame if the loss is small. The existence of an intermediate range of heat loss, between the flame ball and planar flame regimes, within which the expanding spherical flame quenches therefore reveals a very different critical phenomenon for the establishment of flame balls than that described by Wu et al. [14]. Since these interesting flame responses are inherently unsteady and history sensitive, and must necessarily also depend on the chemical, diffusive, and radiative aspects of the system, it behooves us to conduct a detailed unsteady computational simulation using realistic descriptions of these aspects and explore the possibility that these phenomena indeed exist. We shall also conduct the simulation for H_2/air mixtures, as investigated in the space experiments of STS-83 and STS-94 [16], and demonstrate in due course that these unique flame responses are indeed well described.

The problem studied is defined in the next section, which is followed by presentation and discussion of the results.

Problem Definition

The simulation employed the one-dimensional, time-dependent flame code of Rogg and Wang [17], with detailed chemical, transport, and (optically thin and optically thick) radiation models. Other works [14,16,18] have examined quite extensively the effect of different chemical kinetic models on steady flame balls. Since chemistry is not the main focus of the present work, only a single detailed kinetic mechanism, that of Rogg [19], is applied here.

Using the small Mach number approximation, where the thermodynamic pressure is constant throughout the flow field, the governing equations are as follows:

$$\frac{\partial \rho}{\partial t} + u\frac{\partial \rho}{\partial r} = -\frac{\rho}{r^2}\frac{\partial (r^2 u)}{\partial r} \tag{1a}$$

$$c_p \rho\left(\frac{\partial T}{\partial t} + u\frac{\partial T}{\partial r}\right) = \frac{1}{r^2}\frac{\partial}{\partial r}\left(r^2\lambda\frac{\partial T}{\partial r}\right) - \sum_{i=1}^{N} h_i\omega_i - \frac{\partial T}{\partial r}\sum_{i=1}^{N} c_{p,i} j_i - q_{rad} + q_e \tag{1b}$$

$$\rho\left(\frac{\partial Y_i}{\partial t} + u\frac{\partial Y_i}{\partial r}\right) = -\frac{1}{r^2}\frac{\partial (r^2 j_i)}{\partial r} + \omega_i \tag{1c}$$

$$p = \frac{\rho R T}{M} \tag{1d}$$

where t is the time, r is the radius, u is the radial velocity, ρ is the density, T is the temperature, c_p and λ are the constant-pressure heat capacity and thermal conductivity of the mixture, respectively, p is the pressure, R is the universal gas constant, M is the mass averaged molecular weight of the mixture, and N is the total number of species. Furthermore, Y_i, ω_i, h_i, and j_i are the mass fraction, the mass rate of production, the specific enthalpy, and the mass diffusion flux of the ith species, respectively.

For optically thin radiation

$$q_{rad} = 4\alpha_p \sigma (T^4 - T_\infty^4) \tag{2}$$

where σ is the Stefan-Boltzmann constant and α_p is the total Planck mean absorption coefficient. Radiation heat loss is considered to be emitted only from H_2O. Planck mean absorption/emission coefficients of Hubbard and Tien (H&T) [20], based on a wide-band model, are compared with those of Ju et al. [21], based on a statistical narrowband (SNB) model.

For optically thick radiation, radiative transport including both emission and absorption is computed using the SNB model with exponential-tailed inverse line strength distribution [22]. The radiative transfer equations are solved for wave numbers between 150 and 9300 cm^{-1} with 25 cm^{-1} resolution using the S6 discrete ordinate method. Radiation parameters for H_2O are taken from Ref. [23].

Ignition is achieved by energy deposition centered at zero radius, such that

$$q_e = \frac{\Delta}{\tau_s}\exp\left[-\left(\frac{r}{r_s}\right)^8\right] \qquad t \le \tau_s \tag{3}$$

$$q_e = 0 \qquad t > \tau_s$$

where Δ is the density, r_s is the radius, and τ_s is the duration of the source energy. A typical ignition energy is 30 mJ, which is comparable to those used in earlier simulations and experimentation. Different localized ignition kernels of reasonable temporal and spatial size were tested, and as found in Ref. [15], the flame responses are independent of the ignition source, after a rapid transient period. It is conceivable that large ignition kernels can affect flame ball formation for mixture compositions bordering the self-quenching flame regime, to be discussed in detail later, pushing them into that regime. Otherwise, the results confirm that the phenomenon is controlled by the dynamics of the flame front instead of the ignition energy.

At $r = 0$, zero-gradient conditions are enforced. At the ambience side, boundary conditions imposed are temperature, T_∞, fixed mixture composition, and

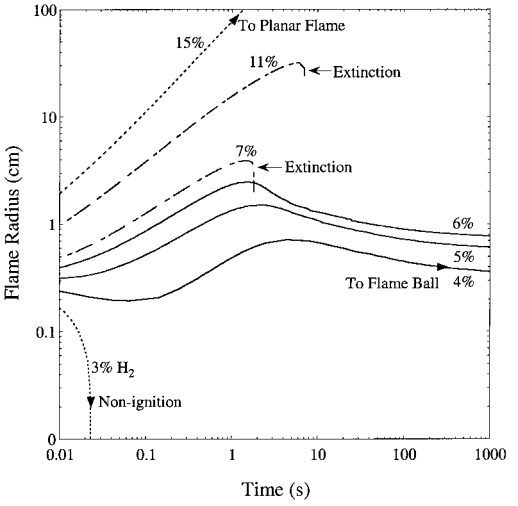

FIG. 1. Flame radii (corresponding to the position of maximum heat release) as a function of time for different molar percentages of hydrogen in air. Calculations assume optically thin radiative heat loss employing the Planck mean absorption/emission coefficients of Hubbard and Tien [20].

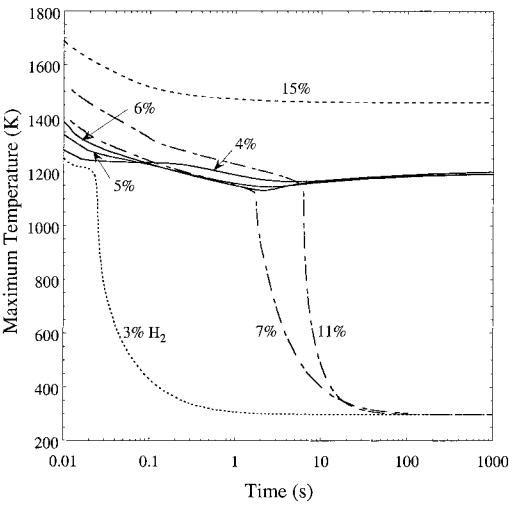

FIG. 2. Maximum flame temperatures as a function of time, corresponding to Fig. 1, for different molar percentages of hydrogen in air. Calculations assume optically thin radiative heat loss employing the Planck mean absorption/emission coefficients of Hubbard and Tien [20].

radiative emissivity of unity. An outer boundary radius of 1 m is used.

Results and Discussion

Phenomena and Concentration Limits

For simplicity in presenting the role of radiative heat loss on the dynamics of flame ball formation, the results given in this section are based on calculations employing optically thin radiation with the Planck mean absorption/emission coefficients of Hubbard and Tien [20]. With respect to the scope of this work, the effects of reabsorption are mainly quantitative and do not affect the discussion of the underlying physical mechanisms. Nonetheless, details of the quantitative effects of different radiation models are discussed in a subsequent section.

We also note that while the study of He and Law [15] was conducted by varying the extent of heat loss, this parameter is hard to control in real systems. Since the phenomena here are basically consequences of the relative magnitudes of heat generation and loss, we have used hydrogen concentration, in lean mixtures, as the system variable to track the flame response, as was done in, for example, Ref. [14].

The flame radius, defined as the location of peak heat release, is plotted in Fig. 1 as a function of time for different concentrations of H_2 in air. The corresponding maximum flame temperature is plotted in Fig. 2. It is first seen that, with 3% H_2 in air, the mixture is below the (lean) ignition limit. It is further found that even under adiabatic conditions, without radiative loss, a self-propagating spherical flame cannot be established from a finite ignition source for hydrogen concentrations smaller than this limit, and any movement of the heat release front is supported by this external ignition source.

Above the ignition limit, we first encounter a narrow range of mixture composition within which flame balls are formed. Particularly in the approximate range of 3.5% to 6.5% H_2, Fig. 1 shows that a spherical flame initially propagates outwardly but then recedes inwardly, with a negative flame speed, as it slowly evolves into a flame ball with a steady-state flame radius. The relaxing process to achieve the flame ball state is, however, exceedingly slow, which is characteristic of diffusion-dominated processes. Figs. 1 and 2 show that there is still substantial change in the flame radius after 10 to 100 s of propagation time. Even at 1000 s, which is the end of the computation time, the flame structure is still much thinner than that of a steady-state flame ball.

With further increase in the hydrogen concentration, it is seen that flame balls can no longer be established (e.g., in 7% H_2), and the expanding spherical flame propagates until it self-extinguishes due to radiative loss from its large volume, as evidenced by the rapid drop in the maximum temperature. For higher hydrogen concentrations (e.g., 11%), the propagation persists to larger flame radii before self-extinction.

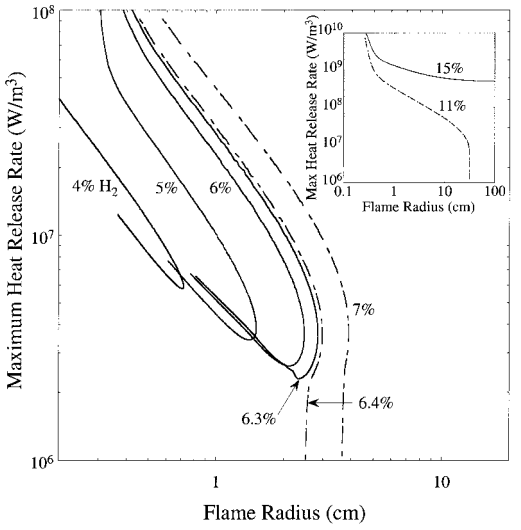

FIG. 3. Maximum chemical heat release rates at the flame's instantaneous radius, corresponding to Figs. 1 and 2, for different molar percentages of hydrogen in air. The inset shows the 11% and 15% hydrogen-in-air cases. The maximum heat release rate of 10^6 W/m^3 serves as the cutoff for flames that extinguish, with the subsequent heat release rates approaching zero.

With even higher hydrogen concentrations (e.g., 15%), the flame burns stronger and the propagation is eventually able to survive permanently in spite of the radiative loss, evolving asymptotically to a planar flame.

Figure 2 also shows that after ignition, the maximum temperature decreases as the flame expands outwardly. For the 15% H_2 case, the flame temperature continuously decreases to that of the planar flame. This is consistent with the properties of $Le < 1$ flames because the flame is subjected to decreasing magnitudes of positive stretch as it propagates outward. For the self-extinguishing flame, increasing radiative loss eventually prevents continued outward propagation of the flame, and the flame temperature drops precipitously, as just observed. For the flame ball case, however, at the initial decrease in the flame temperature, it subsequently increases on reversal in its flame motion direction and eventually attains the steady-state temperature of the flame ball. It is therefore reasonable to anticipate a fundamental change in the flame structure accompanying such a drastic, non-monotonic switch over in the flame response.

Figures 1 and 2 show that qualitative changes in the responses of the self-extinguishing flames and flame ball–forming flames occur around the state when the originally outwardly expanding flame reverses its direction of motion. To further clarify the differences in the flame responses for these two modes of propagation, Fig. 3 plots the maximum heat release rate as a function of the instantaneous flame radius. It is seen that shortly after the flame has reversed its direction of motion, as indicated by the turning point in the response curve, the flame behavior bifurcates for a hydrogen concentration between 6.3% and 6.4%, with those higher than 6.4% fated for extinction and those lower than 6.3% evolving into flame balls. At the turning point, the flame speed changes from positive to negative, and the flame is in a sense an unsteady flame ball because convection vanishes momentarily and the flame process is that of transient diffusion. It is therefore reasonable to interpret this turning point as the transition state at which radiative loss has sufficiently slowed down the flame and modified its structure from that characteristic of a propagating flame to that characteristic of a flame ball. However, the flame temperature immediately after the turning point is still high, and reaction continues at a significant rate. Subsequently, for richer mixtures with larger flame sizes (6.4%–11%), volumetric radiative loss overcomes heat release, and the flame extinguishes. By the same reasoning, for leaner mixtures with smaller flame sizes, heat release from the evolving diffusive flame structure is able to exceed radiative loss, and the flame temperature now again increases due to the Lewis number effect. A flame ball is therefore created.

There are several additional points worth noting. First, while the state of the flame shrinkage is a turning point, it is a manifestation of a non-monotonic behavior in the flame response and is therefore not a flame extinction turning point. Second, since extinction has obviously occurred subsequent to the precipitous drop in the reaction rate, the flame radius here is simply the location of the mixing layer interface, between the combustion product and the fresh reactant, at which some residue reaction of negligible magnitude takes place.

The stability analysis of the steady-state flame ball [14], also using the optically thin approximation, shows that stable flame balls can exist up to 10.7% H_2. This is much beyond the present concentration limit of about 6.4%, obtained through the dynamic simulation of the entire growth history of the propagation flame. Such a significant difference highlights the inadequacy of stability analysis based on a state which is not dynamically accessible itself, if the ignition source is localized and produces an initial flame kernel which is much smaller than that of the $1/r$ flame structure of the flame ball, which in fact contains an infinite amount of thermal energy. Simulations also have been run with ignition kernels of sizes comparable to those of steady flame ball radii, with the same transient dynamics occurring, further verifying that certain flame balls are not dynamically attainable, unless of course they are initially formed with structures similar to those of the steady state.

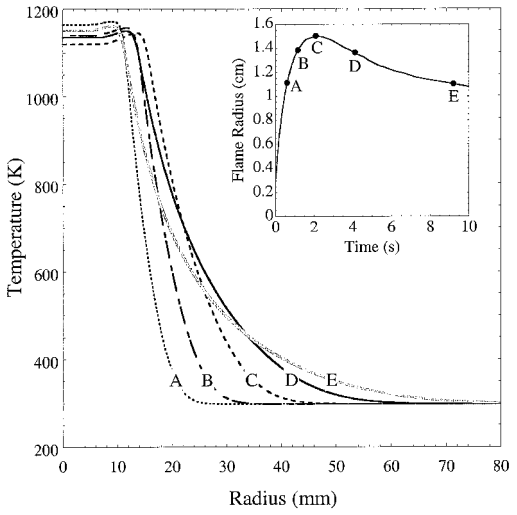

FIG. 4. Profiles of temperature for the 5% hydrogen-in-air flame at different times as it evolves into a flame ball. The corresponding temporal position for each of the temperature profiles can be extrapolated from the inset.

As mentioned earlier, the ignition limit of 3.5% H_2 turns out to be about the same with and without radiative loss, provided that the ignition source is localized. The fact that these mixtures are not ignitable even under adiabatic conditions implies that although steady, adiabatic, planar flames can exist in the doubly infinite domain for mixture compositions below this limit, they cannot be dynamically attained from initially localized flame structures. As such, this concentration ignition limit can be identified as the lean flammability limit of the mixture for situations involving ignition kernels. The concept of the existence of stable, steady flames which may not be dynamically realized from a localized initial structure is directly analogous to ours for the limited dynamic range of flame ball formation.

Evolvement of Flame Structure

We next study the structure of the flame as it evolves into the flame ball. Figs. 4 and 5 display elements of the flame structure (temperature, H_2O product mole fraction, heat release rate, and radiative loss rate) at different points in the physical and phase trajectories of the flame ball (see insets) for the 5% H_2 case. For points A–C, where C corresponds to the maximum attained flame radius, the flame structure, in terms of the diffusive properties of temperature and H_2O concentration, is that of the conventional propagating premixed flame with a localized structure, characterized by exponential decay of the profiles. At point D, which has the same flame radius as that of point B, the flame structure is seen to be very different from that of points A–C in that it now has a $1/r$ character, which is indicative of the purely diffusive nature of the flame ball. This $1/r$ behavior is further crystallized at point E, which has the same flame radius as that of point A. The behavior at points D and E is of course not strictly $1/r$ because the flame is still very far from its steady-state structure and convective effects must be present as the flame moves inwardly. But what is particularly significant is the dramatic change in flame structure as it evolves from a localized, exponential one for a propagating premixed flame into a diffusive, $1/r$ one for the flame ball.

The heat release profiles show that the heat release zone remains thin even as the flame takes on a more diffusive structure. This is reasonable because convection is of a higher-order influence in the reaction zone. It is also of interest to note that while the flame temperature in the reaction zone is fairly close for all states, and that states B and D and states A and E have the same radius, the heat release rate is higher for the expanding, propagating-flame phase than it is for the regressing, flame ball phase. This is caused by the higher rates of reactant diffusion into the reaction zone for the former because the concentration gradient is exponential instead of $1/r$. Similarly, the radiative loss rates are comparatively higher for the flame ball–like flames because the $1/r$ gradient reduces the outward H_2O product diffusion, which then leads to higher concentrations behind the reaction zone.

The results in this section divulge the dual role of radiative loss, which both creates and stabilizes flame balls as well as prevents their existence. Since adiabatic flame balls are not stable, adiabatic calculations confirm that such flames never evolve into flame balls and instead propagate forever, becoming planar flames. Radiative loss is essential in changing the flame structure from a propagating one into one that is optimal for the stabilization and sustenance of a flame ball. At the same time, radiative loss engenders the self-extinguishing flame phenomenon, which prevents their dynamic attainment and defines the boundary between flame balls and planar flames.

Radiative Reabsorption

Calculations were also performed for different radiation submodels—namely, optically thin cases with H&T and SNB parameters and optically thick cases with gas-phase reabsorption using SNB parameters. Fig. 6 shows, for the 5% H_2 case, that the quantitative effect of reabsorption is quite substantial, resulting in an evolving flame ball (after 1000 s) that is over 25% larger than that for the optically thin case using wideband parameters. Such increases were also obtained for the 4% and 6% H_2 cases.

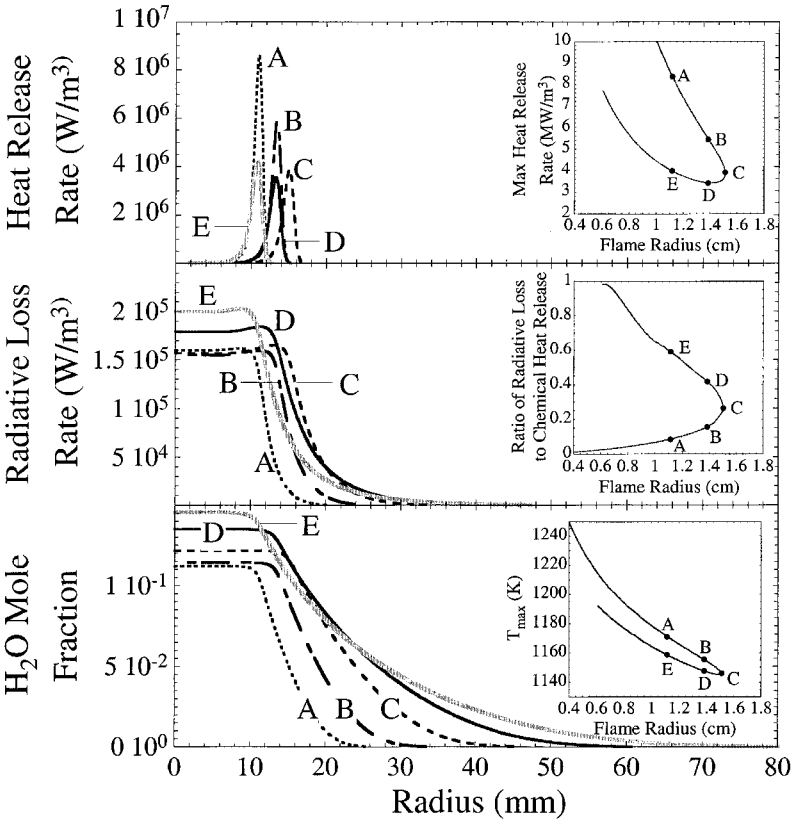

FIG. 5. Profiles of chemical heat release rate per unit volume, radiative heat loss rate per unit volume, and H_2O mole fraction for the 5% hydrogen-in-air flame at different times corresponding to the thermal structures given in Fig. 4. The insets show the corresponding flame responses of maximum heat release rate, ratio of integrated radiative loss rate to heat release rate, and maximum temperature as a function of the instantaneous flame radius.

With H_2O mean Planck absorption length larger than the radius of optically thin calculations for small flame balls (such as 4% H_2), one might expect the effect of reabsorption to be small in this case. However, due to the radial symmetry of the problem, radiation emitted at a given radius is reflected back from center, thereby providing an extended path length for reabsorption. Additionally, by allowing for reabsorption for the same mixture composition, the flame ball becomes larger, which in turn provides extended path lengths for reabsorption. As seen from the inset of Fig. 6, the flame dynamics discussed in the previous section are only quantitatively affected. However, since the attainment of the flame ball depends sensitively on the radiative transfer aspects of the process, which in turn is also coupled to the flame size (notice that the maximum radius is smallest for the reabsorption case), it is reasonable to expect that reabsorption would modify the transition boundaries for the self-extinguishing flames and flame balls. Such mapping calculations are computationally intensive and tedious and are outside the scope of the present investigation.

Experiments presented in other works [16,24] show that numerical calculations for H_2/air mixtures often underpredict experimental flame ball sizes. Fig. 7 compares computed flame ball radii for steady and transient cases along with experimental data [24]. The results of this work show that inclusion of radiative reabsorption can increase the flame size. Additionally, since the experiments are inherently transient, with a local ignition source, experimental time durations (around 500 s maximum) may not be sufficient to compare with steady-state values. We also note that the simulations are based on the chemical kinetic mechanism of Rogg [19], which has been shown to predict steady flame ball sizes up to 50% smaller than other chemical kinetic mechanisms [24]. As a result, transient calculations with reabsorption with other chemical kinetic mechanisms could bring the calculated values closer to the experimental data.

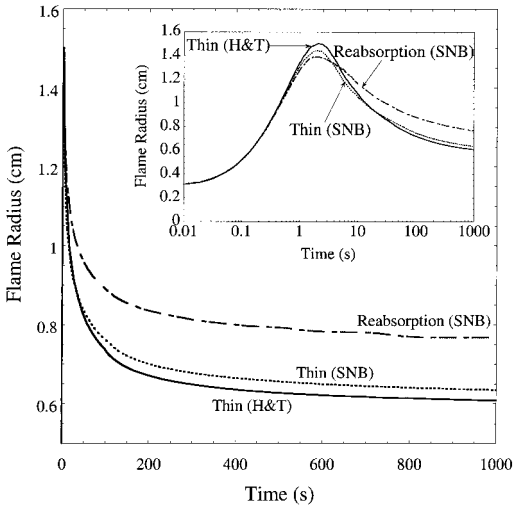

FIG. 6. Flame radii (corresponding to the position of maximum heat release) of 5% hydrogen in air as a function of time for three different radiative cases. The inset shows the same trajectories on a semi-log scale.

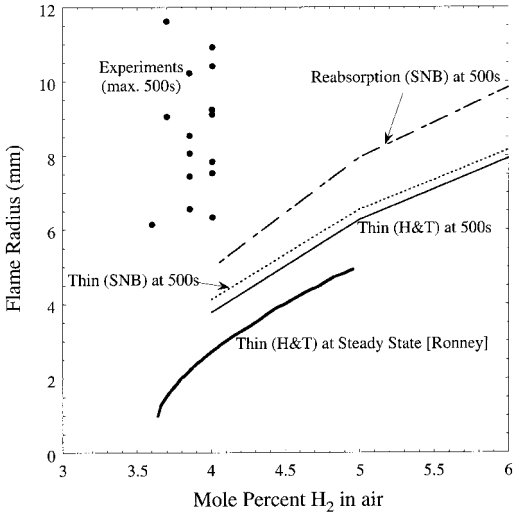

FIG. 7. Comparison of flame ball radii after 500 s of evolution for three different radiative models, along with the experimental results and steady-state calculated results of Ronney [24]. The shown calculations of Ronney and of this work employ the same chemical mechanism [19].

Concluding Remarks

This work has conclusively identified the mechanisms and factors responsible for the formation of a flame ball from a centrally ignited premixture. Moreover, the analyses and simulations evince that flame balls can be established from a propagating premixed flame for only a narrow range of mixtures, narrower than the range for which stable, steady flame balls exist and consistent with that found in experiments. Radiative loss is responsible for both the creation and non-creation of flame balls for different mixture compositions. Radiative reabsorption effects are likely to modify the dynamic and static ranges for which flame balls may be achieved. Nonetheless, it is the self-extinguishing flame phenomenon which limits the dynamic range from the static one and also exists as the mechanism which separates flame balls from planar flames.

Previous analyses have found stationary flame balls to be unstable to three-dimensional perturbations [25]. However, since the present work has shown that flame balls are a continuous extension of propagating flames of very different flame structure from an ignition source, further analysis is needed to study the impact of these multidimensional effects during the transient stage while the flames are still developing. It is not clear if such three-dimensional instabilities (applied for steady-state flame structures) can induce the flame ball breakup phenomenon found in experiments prior to possible multidimensional manifestation of the mechanism described in this work. As a result, further investigation is needed to determine the influence of the three-dimensional effects on the true path of flame ball formation from ignition.

Acknowledgments

This work was supported by NASA under its Microgravity Combustion Program. Special thanks are due to Professor P. D. Ronney, of the University of Southern California, for his helpful advice and discussions, and to Dr. Y. Ju, of Princeton University, for his help with the reabsorption calculations.

REFERENCES

1. Frankel, M. L., and Sivashinsky, G. I., *Combust. Sci. Technol.* 31:131–138 (1983).
2. Pelce, P., and Clavin, P., *J. Fluid Mech.* 124:219–237 (1982).
3. Sun, C. J., Sung, C. J., He, L., and Law, C. K., *Combust. Flame* 118:108–128 (1999).
4. Zeldovich, Ya. B., "Theory of Combustion and Detonation of Gases," in *Selected Works of Yakov Borisovich Zeldovich* (J. P. Ostriker, G. I. Barenblatt and R. A. Sunyaev eds.), Izd-vo. Akad. Nauk USSR, Moscow, 1992 pp. 162–232.
5. Zeldovich, Ya. B., Barenblatt, G. I., Librovich, V. B., and Makhviladze, G. M., *The Mathematical Theory of Combustion and Explosions*, Consultants Bureau, New York, 1985.
6. Deshaies, B., and Joulin, G., *Combust. Sci. Technol.* 37:99 (1984).

7. Buckmaster, J., Joulin, G., and Ronney, P., *Combust. Flame* 79:381–392 (1990).
8. Buckmaster, J., Joulin, G., and Ronney, P., *Combust. Flame* 79:411–422 (1991).
9. Ronney, P. D., *Combust. Flame* 82:1–14 (1990).
10. Ronney, P. D., Whaling, K. N., Abbud-Madrid, A., Gatto, J. L., and Pisowicz, V. L., *AIAA J.* 32(3):569–577 (1994).
11. Lozinski, D., Buckmaster, J., and Ronney, P., *Combust. Flame* 97:301–316 (1994).
12. Buckmaster, J. D., Smooke, M. D., and Giovangigli, V., *Combust. Flame* 94:113–124 (1993).
13. Smooke, M. D., and Ern, A., NASA Conference Publ. 10174, Cleveland, OH, pp. 445–450, 1995.
14. Wu, M. S., Ronney, P., Colantonio, R. O., and Vanzandt, D. M., *Combust. Flame* 116:387–397 (1999).
15. He, L., and Law, C. K., "On the Dynamics of Transition from Propagating Flame to Stationary Flame Ball," AIAA paper 99-0325, *Thirty-Seventh Aerospace Sciences Meeting and Exhibit,* AIAA, Reno, NV, January 11–14, 1999.
16. Wu, M. S., Liu, J. B., and Ronney, P. D., *Proc. Combust. Inst.* 27:2543–2550 (1998).
17. Rogg, B., and Wang, W., *RUN-1DL: The Cambridge Universal Flamelet Computer Code, User Manual,* University of Cambridge, Cambridge, England (1995).
18. Abid, M., Wu, M. S., Liu, J. B., Ronney, P. D., Ueki, M., Maruta, K., Kobayashi, H., Niioka, T., and Vanzandt, D. M., *Combust. Flame* 116:348–359 (1999).
19. Rogg, B., in *Reduced Kinetic Mechanisms for Applications in Combustion Systems,* (N. Peters, and B. Rogg, eds.), Springer-Verlag, Berlin, 1993, Appendix C.
20. Hubbard, G. L., and Tien, C. L., *J. Heat Transfer* 100:235–239 (1978).
21. Ju, Y., Guo, H., Liu, F., and Maruta, K., *J. Fluid Mech.* 379:165–190 (1999).
22. Malkmus, W., *J. Opt. Soc. Am.* 57:323–329 (1967).
23. Soufinani, A., and Taine, J., *Int. J. Heat Mass Transfer* 40:987–991 (1997).
24. Ronney, P. D., *Proc. Combust. Inst.* 27:2485–2506 (1998).
25. Buckmaster, J., Gessman, R., and Ronney, P., *Proc. Combust. Inst.* 24:53–59 (1992).